Soft Matter

PAPER

Cite this: *Soft Matter*, 2018, **14**, 2322

Effect of HU protein on the conformation and compaction of DNA in a nanochannel

Durgarao Guttula,[a] Fan Liu,[a] Jeroen A. van Kan,[a] Véronique Arluison[bc] and Johan R. C. van der Maarel*[a]

Received 27th October 2017,
Accepted 10th February 2018

DOI: 10.1039/c7sm02118f

rsc.li/soft-matter-journal

The effect of the heat unstable nucleoid structuring protein HU on the conformation of single DNA molecules confined in a nanochannel was investigated with fluorescence microscopy. Pre-incubated DNA molecules contract in the longitudinal direction of the channel with increasing concentration of HU. This contraction is mainly due to HU-mediated bridging of distal DNA segments and is controlled by channel diameter as well as ionic composition and strength of the buffer. For over-threshold concentrations of HU, the DNA molecules compact into an condensed form. Divalent magnesium ions facilitate, but are not required for bridging nor condensation. The conformational response following exposure to HU was investigated with a nanofluidic device that allows an *in situ* change in environmental solution conditions. The stretch of the nucleoprotein complex first increases, reaches an apex in ~20 min, and subsequently decreases to an equilibrium value pertaining to pre-incubated DNA molecules after ~2 h. This observation is rationalised in terms of a time-dependent bending rigidity by structural rearrangement of bound HU protein followed by compaction through bridging interaction. Results are discussed in regard to previous results obtained for nucleoid associated proteins H-NS and Hfq, with important implications for protein binding related gene regulation.

1 Introduction

HU is one of the most abundant nucleoid associated proteins (NAPs) and plays a pivotal role in the compaction, transcription, and replication of the bacterial genome. It is present throughout the growth cycle with up to one HU per 300–400 base pairs in the log phase.[1,2] The functioning of HU and other NAPs such as H-NS and Hfq is not clearly understood, but they are known to induce structural changes in DNA and DNA assemblies. The functional unit of HU is a dimer of two subunits HU_α and HU_β with a total molecular weight of ~18 kDa and an isoelectric point pI of 9.5. The heterodimer $HU_{\alpha\beta}$ is the predominant form and has the highest, sequence unspecific affinity to double stranded DNA.[3–5] Binding of HU results in a kink and under-winding of the duplex by the insertion of two proline residues separated by nine base pairs along the contour.[6,7] At lower concentrations of HU ($\leq$50 nM), the HU–DNA complex is more flexible compared to bare DNA because of HU induced bending of the duplex. At higher concentrations of HU, a nucleoprotein filament is formed with about one HU dimer per nine base pairs.[8–11] The bending rigidity of this filament depends on the time the DNA is exposed to HU. The complex first becomes stiff, but regains the flexibility of bare DNA after ~2 h. This time-dependence was rationalised in terms a structural rearrangement of bound HU on DNA, resulting in a change in topology, an increase in bending flexibility and an increase in contour length through a decrease in helical pitch of the duplex.[12] The filaments can assemble into a periodic network by HU-mediated bridging interaction that controls compaction of the nucleoid in the growth phase.[13]

Advances in nanofabrication have made it possible to make quasi one-dimensional channel devices with cross-sectional diameters of tens to hundreds of nanometers. Our chips are made of polydimethylsiloxane (PDMS) cast on a high quality master stamp, obtained by proton beam writing and UV lithography.[14,15] About a hundred replicas can be made with a single stamp, so that we have used a fresh chip for every experiment. These channel devices can be used to study the conformation, folding, and compaction of single DNA molecules.[16–18] Confinement in a nanospace results in significant modification of certain important biophysical phenomena, such as the knotting probability of circular DNA and the effect of macromolecular crowding.[19–21] In particular, it was shown that DNA can be condensed into a tightly packed state

[a] *Department of Physics, National University of Singapore, Singapore 117542, Singapore. E-mail: johanmaarel@gmail.com; Fax: +65 6777612; Tel: +65 65164396*
[b] *Laboratoire Léon Brillouin, CEA, CNRS, Université Paris Saclay, 91191 Gif-sur-Yvette, France*
[c] *Université Paris Diderot, Sorbonne Paris Cité, 75013 Paris, France*

for over-threshold concentrations of a crowding agent such as dextran or like-charged proteins.[19,22] Compaction and condensation of DNA with NAPs (H-NS and Hfq) have also been reported before.[23–25] Here, we report the effect of HU in conjunction with confinement inside a nanochannel on the conformation and compaction of DNA. For this purpose, we have done two closely related series of experiments. In the first series, we focus on equilibrium properties of DNA molecules that have been pre-incubated with HU. In the second series, the dynamic conformational response of single DNA molecules following exposure to HU is investigated. Super-resolution imaging of HU in *Escherichia coli* has shown that it is clustered within the nucleoid with a diameter of a few hundred nanometers.[26] This diameter is comparable to the cross-sectional diameters of our channel systems (200–250 nm). Accordingly, we surmise that results for nanochannel confined DNA have implications for gene regulation and chromosome organisation in the bacterial nucleoid.

For the first series of experiments, bacteriophage T4-DNA (166 kbp) is incubated in buffers of various ionic strength and with various concentrations of HU for at least 24 h. Some of the buffers also contained magnesium ions. The DNA molecules were stained with YOYO-1 with an intercalation ratio of 100 base-pairs per dye molecule. For such a low level of intercalation, the distortion of the secondary DNA structure is minimal. Furthermore, there is no appreciable effect on the bending rigidity, as inferred from previously reported measurements of the extension of DNA in nanochannels with different concentrations of dye.[16] The pre-incubated molecules are driven into a single array of nanochannels with the help of an electric field. Once the molecules are equilibrated after switching off the electric field, their extensions along the direction of the channel (stretch) are measured with fluorescence microscopy.

The second series of experiments focuses on the dynamic response following exposure to HU in a cross-channel set up.[27] As shown by the layout of the device in Fig. 1, a centrally located grid of rectangular nanochannels is connected to two sets of microchannels with loading reservoirs. The grid features two arrays of parallel nanochannels in a perpendicular configuration. The cross sections of the channels pertaining to the respective arrays are 150 × 200 and 200 × 250 nm^2. DNA immersed in the relevant buffer, but without HU, was driven into the device through the array of wider channels in one direction with the help of an electric field. Once the molecules were equilibrated inside the channels after switching off the field, a buffered solution of HU was pipetted into one of the reservoirs of the other set of microchannels. The protein subsequently diffuses through the intersecting array of nanochannels and uniformly penetrates the array of wider channels. During and following exposure to HU, the conformational response of the DNA molecules was monitored with fluorescence microscopy.

Our observations are analysed in terms of the architectural properties of HU; in particular the formation of a nucleoprotein filament and HU-mediated assembling into a periodic network. We will also compare our results with those previously obtained for H-NS and Hfq, highlighting differences and similarities between these relatively abundant NAPs in shaping the bacterial genome.

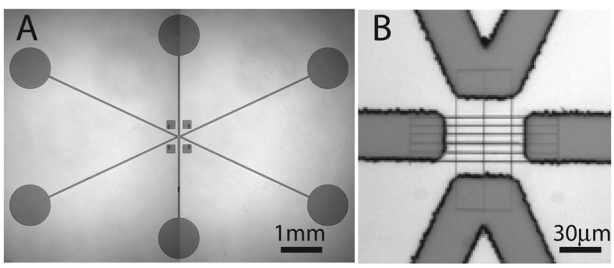

Fig. 1 (A) Bright field optical image of the cross-channel device. The reservoirs are connected to the grid of nanochannels by microchannels. (B) Optical image of the master stamp showing the nanochannels with connecting microchannels. The nanochannels have a uniform height of 200 nm and widths of 250 and 150 nm in the two perpendicular directions, respectively. The wide and narrow channels are laid on a rectangular grid and separated by 6 and 20 μm, respectively.

2 Materials and methods

2.1 Isolation and purification of HU

pETDuet-1 HU plasmid, which has been designed for co-expressing HU_α (*hupA* gene) with N-terminal his6-tag and HU_β (*hupB* gene), was transformed into *Escherichia coli* BL21(DE3) cells. The cells were grown at 310 K in Luria Broth medium containing ampicillin and the overproduction of HU was induced by adding 4 mM IPTG at 293 K. The cells were lysed by sonication in 10 mM Tris–HCl, pH 8 buffer containing 250 mM NaCl and 10% glycerol. The lysate was cleared by centrifugation at 35 000 rpm for 30 min at 277 K. The lysate was then diluted with the same buffer and loaded into a HisTrap HP column (GE healthcare). The column was eluted with an imidazole gradient. The protein was further purified by using a Superdex 75 gel filtration column and dispersed in a buffer comprising 500 mM KCl and 10 mM Tris–HCl, pH 7.5. The concentration was determined by UV absorbance at 230 nm with A_{230} = 2.3 per 1 g of HU per L.[28]

2.2 Sample preparation

T4 GT7 DNA (T4-DNA, 165.65 kbp) was purchased from Nippon Gene, Tokyo and used without further purification. The integrity of T4-DNA was verified with pulsed gel electrophoresis. No fragments of one to tens of kbps were observed. Samples were prepared by dialysing solutions of DNA against 10 mM Tris–HCl with the relevant concentration of NaCl and/or $MgCl_2$ in microdialysers. Solutions of HU in the same buffer were also prepared. The Tris–HCl concentration is 10 mM Tris adjusted with HCl to pH 7.5, (T-buffer, that is 8.1 mM TrisCl and 1.9 mM Tris). The ionic strength of the buffer was calculated with the Davies equation for estimating the activity coefficients of the ions and a dissociation constant pK = 8.08 for Tris. For the measurement of the pre-equilibrated DNA molecules, solutions of HU and DNA were subsequently mixed and incubated overnight at 277 K. YOYO-1 fluorescence staining dye was

purchased from Invitrogen, Carlsbad, CA. T4-DNA was stained with YOYO-1 with an incubation time of 24 h and an intercalation ratio of 100 base-pairs per dye molecule. No anti-photo bleaching agent was used, since it might interfere with DNA–protein binding. The final concentration is 3 mg of DNA per L.

2.3 Fabrication of the nanofluidic chips

The nanofluidic devices were fabricated by replication in PDMS of patterned master stamps.[15,16] The nanochannels were made in HSQ resist (Dow Corning, Midland, MI) using a lithography process with proton beam writing.[14] Chips with two different channel layouts were made. For the measurement of the pre-incubated DNA molecules, a single array of nanochannels is connected to two loading reservoirs through a superposing set of microchannels made in SU-8 resin with UV lithography. For the investigation of the response to a change in solution conditions, a cross-channel device was made (Fig. 1). In the latter device, there are two intersecting arrays of nanochannels connected to two sets of microchannels with loading reservoirs. The heights and widths of the positive channel structures on the stamps were measured with atomic force microscopy (Dimension 3000, Veeco, Woodbury, NY) and scanning electron microscopy, respectively. For the single-array device, two stamps were made featuring nanochannels of length 60 μm and rectangular cross-sections of 150 × 250 and 200 × 300 nm^2, respectively. The cross-sections pertaining to the two intersecting arrays of the cross-channel device are 150 × 200 and 200 × 250 nm^2. The connecting microchannels have a width and height of 30 and 5 μm, respectively. The stamp was coated with a 5 nm thick teflon layer to guarantee perfect release of the replicated PDMS chips.[29] The stamps were replicated in PDMS followed by curing with a curing agent (Sylgard, Dow Corning) at 338 K for 24 h. The PDMS replica was sealed with a glass coverslip, after both substrates were plasma oxidised (Harrick, Ossining, NY).

2.4 Single-channel array

The pre-incubated and stained DNA molecules dispersed in the relevant solution were loaded into one of the two reservoirs connected to the single array of nanochannels. The DNA molecules were subsequently driven into the channels by electrophoresis. For this purpose, two platinum electrodes were immersed in the reservoirs and connected to an electrophoresis power supply with a relatively low voltage in the range 0.1–10 V (Keithley, Cleveland, OH). Once the DNA molecules were localised inside the nanochannels, the electric field was switched off and the molecules were allowed to relax to their equilibrium state for at least 60 s. The stained DNA molecules were visualised with a Nikon Eclipse Ti inverted fluorescence microscope equipped with a 200 W metal halide lamp, a filter set, and a 100× oil immersion objective. A UV light shutter controlled the exposure time. Images were collected with an electron multiplying charge coupled device (EMCCD) camera (iXon X3, Andor Technology, Belfast, UK) and the extension of the DNA molecules inside the channels was measured with imageJ software (http://rsb.info.nih.gov/ij/). For intensity threshold, we have used two times the signal to background noise ratio.

2.5 Cross-channel array

The protein-free, stained DNA molecules were loaded into the reservoirs connected to the array of 200 × 250 nm^2 nanochannels. To maintain the balance in pressure, T-buffer (without DNA) was loaded into the other reservoirs connected to the perpendicular, intersecting array of 200 × 150 nm^2 channels. The DNA molecules were subsequently driven into the channels by electrophoresis and allowed to relax for at least 60 s as described above. At pre-set times, solutions of HU are flushed through one of the microchannels of the other set with a syringe. The protein is subsequently transported through the intersecting array of 200 × 150 nm^2 into the 200 × 250 nm^2 nanochannels by diffusion. During and following exposure to HU, the stained DNA molecules were visualised and their extensions were analysed as described above.

3 Results

3.1 Pre-incubated DNA

In the first series of experiments, T4-DNA molecules were incubated with the relevant solution of HU for at least 24 h before they were brought into the channels of the single-array device. Montages of images of single DNA molecules confined in rectangular channels with a cross-section of 200 × 300 nm^2 are shown in Fig. 2. The images refer to well-equilibrated conformations. After the electric field is switched off, the molecules relax to their equilibrium state within 60 s. We have

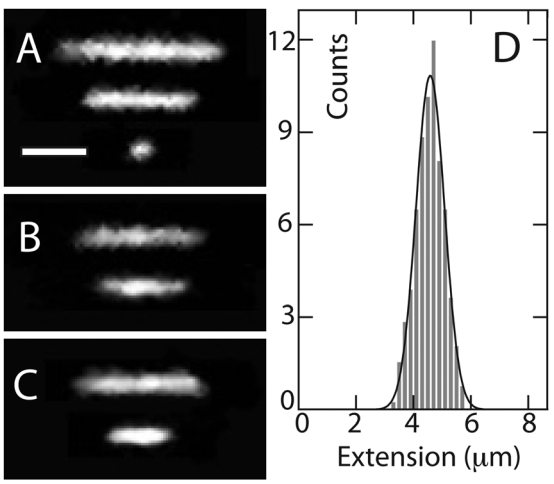

Fig. 2 (A) Montage of fluorescence images of T4-DNA in T-buffer with 3 mM NaCl and inside 200 × 300 nm^2 channels. T-buffer is 8.1 mM TrisCl and 1.9 mM Tris, pH 7.5. The HU concentration is 10, 100, and 400 nM from top to bottom. The scale bar denotes 3 μm. (B) As in panel (A), but in T-buffer with 30 mM NaCl. The HU concentrations are 10 and 30 nM from top to bottom. (C) As in panel (A), but in T-buffer with 3 mM NaCl and 0.4 mM $MgCl_2$. The HU concentrations are 10 and 80 nM from top to bottom. (D) Distribution in extension of a population of 80 molecules in T-buffer with 3 mM NaCl and 100 nM HU, inside 200 × 300 nm^2 channels. A Gaussian fit gives $R_{\|}$ = 4.5 ± 1.0 μm.

verified that there is no further change in extension for more than 3 h. Furthermore, we observed no difference in extension between molecules inserted by electrophoresis or pressure. Irrespective of buffer conditions, the equilibrated stretch in the longitudinal direction of the channel decreases with increasing concentration of HU. For over-threshold concentrations of HU, condensation of DNA into a tightly packed form is observed. Condensed DNA is visible as a bright fluorescence spot of resolution-limited size and can easily be discerned from the extended form. In channels with a smaller cross-section of 150 × 250 nm^2, we observed the same qualitative behaviour. There are quantitative differences however in the values of the stretch and critical concentrations of HU for condensation.

We have measured the extension of the DNA molecules in channels with two different cross-sections: 200 × 300 and 150 × 250 nm^2. For each experimental condition, that is buffer composition, channel diameter, and HU concentration, we have used a fresh PDMS replica and measured around 50 molecules. The distribution in extension is close to Gaussian.[30] An example of such a distribution is shown in Fig. 2D. Fragmented DNAs are discerned by their extension being less than the mean value minus two times the standard deviation. Resolution broadening can be neglected, because the optical resolution is one order of magnitude smaller than the variance. The mean relative extension $R_\parallel/L$, that is the mean extension divided by the YOYO-1 corrected contour length of 57 μm, is set out in Fig. 3 as a function of the HU concentration. With increasing concentration of HU, the DNA molecules contract. The extension also decreases with increasing ionic strength of the buffer. In the presence of 0.4 mM $MgCl_2$, the same qualitative behaviour is observed. Note that for sub-threshold concentrations of HU the relative extensions are in the range 0.05–0.25, which implies that the DNA molecules remain coiled. Furthermore, an increased stretch is observed in the 150 × 250 nm^2 channel system related to the stronger confinement.

For over-threshold concentrations of HU, the DNA molecules compact into a condensed form. This is facilitated by the confinement in the nanochannel, because we did not observe condensation in the feeding microchannels and/or the reservoirs of the chip. To the best of our knowledge, compaction of DNA by HU protein into a condensed form has not been reported before. In 200 × 300 nm^2 channels, the critical concentrations of HU for condensation are 300 ± 50 and 40 ± 10 nM in T-buffer with 3 and 30 mM NaCl, respectively. In the presence of a sub-millimolar concentration of $MgCl_2$, the critical concentration for condensation is shifted downwards from 300 to 90 nM of HU. In the 150 × 250 nm^2 channel system, the critical concentrations of HU are 1.1 ± 0.1 and 5 ± 1 μM in T-buffer with 3 and 30 mM NaCl, respectively. The threshold shifts hence to higher concentrations with decreasing channel cross-sectional diameter.

3.2 Dynamic response

The above described results refer to DNA molecules that were pre-incubated with HU for more than 24 h before they were brought into the nanochannels of the single-array device.

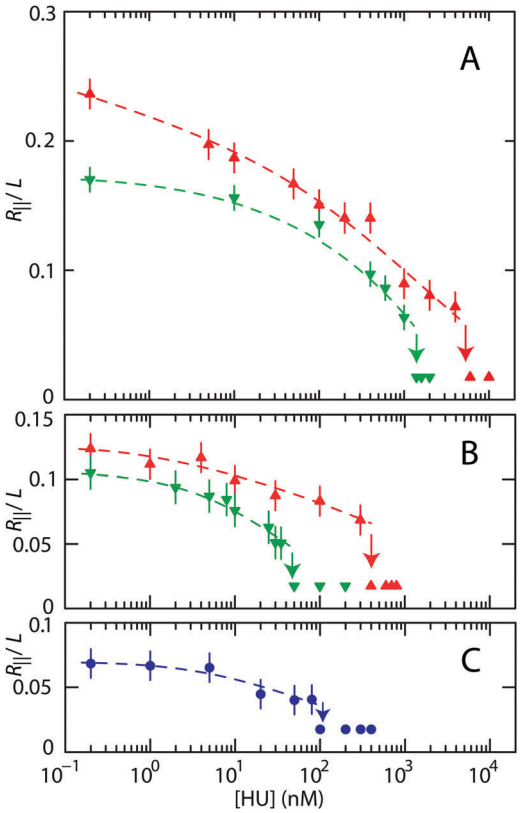

Fig. 3 Relative extension $R_\parallel/L$ of T4-DNA in T-buffer with 3 (red, △) or 30 (green, ▽) mM NaCl *versus* the concentration of HU. The molecules are pre-incubated and inside 150 × 250 nm^2 channels. (B) As in panel (A), but in 200 × 300 nm^2 channels. (C) As in panel (A), but in T-buffer with 3 mM NaCl and 0.8 mM $MgCl_2$ (blue, ○), inside 200 × 300 nm^2 channels. The dashed curves are drawn as an aid to the eye and the arrows denote the condensation thresholds.

In order to obtain more insight in the various mechanisms at hand, we have done a second series of experiments with a cross-channel device. With the latter device, the conformational response of the DNA molecules to a change in environmental solution conditions can be investigated *in situ*.[27] We have used a buffer of moderate ionic strength without magnesium (T-buffer with 3 mM NaCl). Furthermore, we have done two series of experiments with two concentrations of HU (100 and 800 nM) just below the critical concentration for condensation.

Protein-free DNA molecules were brought into the array of wider 200 × 250 nm^2 channels of the cross-channel device by electrophoresis. Once the electric field is switched off, the molecules equilibrate and remain stationary. The initial stretch is 10 ± 1 μm. The HU containing buffer was pipetted into one of the reservoirs of the other set of microchannels and diffused through the intersecting array of the narrower 150 × 200 nm^2 channels into the wider channels. Throughout and following exposure to HU, the DNA molecules are imaged with fluorescence microscopy. The time-dependent stretch after exposure to HU is shown in Fig. 4. A striking result is that the molecules initially elongate. An apex with a maximal extension of about one to two times the extension pertaining to the protein-free state is reached in about 20 min. The maximal elongation

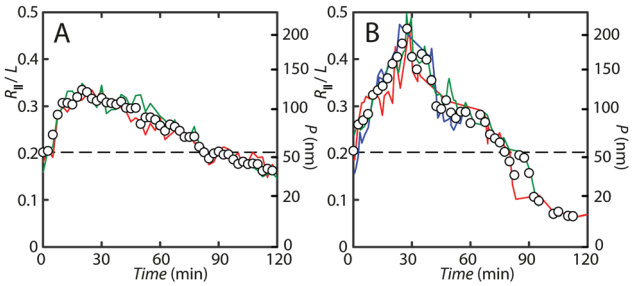

Fig. 4 (A) Temporal change in relative extension $R_{\|}/L$ (left-axis) of T4-DNA following exposure to 100 nM HU in T-buffer with 3 mM NaCl. The molecules are inside 200 × 250 nm^2 channels and, initially, in T-buffer with 3 mM NaCl. (B) As in panel (A), but for 800 nM HU. The symbols represent the average of 2–3 molecules for each concentration of HU, whereas individual trajectories are denoted by the solid curves. The apparent persistence length P is demarcated along the right-axes.

depends on the concentration of HU, with the most pronounced effect observed for the highest employed concentration of 800 nM. For longer times, the stretch reduces and the final, equilibrium state is reached after more than 2 h. Note that the final values of the stretch are less than the value pertaining to the protein-free state, so the molecules eventually contract. The equilibrated values agree with those obtained from 24 h pre-incubated samples, once a small difference in channel cross-sectional diameter has been taken into account.

4 Discussion

4.1 Contraction of pre-incubated DNA

With increasing concentration of HU, pre-incubated DNA molecules contract irrespective of ionic strength and/or composition of the buffer. This observation is strikingly different from a previously reported result for H-NS.[23] The relative extensions of DNA pre-incubated with H-NS, Hfq, and HU are compared in Fig. 5. In the case of H-NS at lower ionic strength (T-buffer with 3 mM NaCl), the DNA molecules are seen to elongate. Elongation can be attributed to an increase in bending rigidity of the protein–DNA complex. Conversely, contraction follows from a decrease in bending rigidity, or, more plausibly, protein-mediated bridging interaction between distal segments of the DNA molecule. The switch between elongation and contraction observed for H-NS indicates that bridging becomes more effective at higher ionic strength. This is possibly related to screening of the electrostatic repulsion between the like-charged segments of the DNA molecule.[23] DNA with sparsely bound HU is more flexible compared to bare DNA. This could explain contraction for concentrations of HU less than 50 nM. At higher HU concentrations, the formation of the nucleoprotein filament results in a temporary increase in bending rigidity.[12] For longer incubation times exceeding 1 h, the corresponding persistence length takes a value of around the value pertaining to bare DNA (~55 nm). Accordingly, the effect of HU on the bending rigidity cannot explain a contraction of the DNA molecule with respect to the protein-free state. A decreased bending rigidity can also not explain the eventual

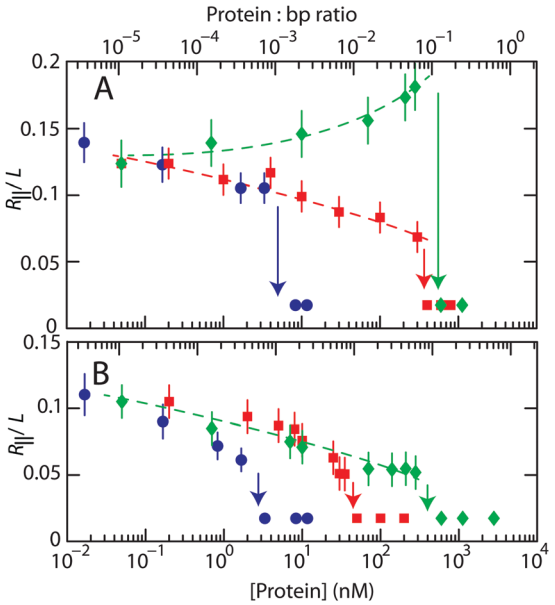

Fig. 5 (A) Relative extension $R_{\|}/L$ of T4-DNA in T-buffer with 3 mM NaCl *versus* the concentration of H-NS (green, ◊),[23] HU (red, □), and Hfq (blue, ○).[24] The molecules are pre-incubated and confined inside 200 × 300 nm^2 channels. (B) As in panel (A), but in T-buffer with 30 mM NaCl.

compaction into a condensed state for over-threshold concentrations of HU. The sub-nominal contraction is hence most likely due to HU-mediated bridging interaction between distal DNA segments. Hfq also binds on DNA, but a rigid filament is not formed.[24,25] Hfq has a strong propensity for bridging, resulting in compaction behaviour similar to HU but with one to two orders lower critical concentrations for condensation (see Fig. 5).

4.2 Temporal stretch

We have investigated the conformational response following exposure to HU with the cross channel device. Qualitatively, similar behaviour is observed for the two employed concentrations of HU. The temporal increase in stretch by a factor of two is most pronounced for the highest concentration of 800 nM. For a wormlike chain with persistence length P and width w inside a channel with diameter $D > P$, Monte Carlo simulation shows that the stretch follows a power law in P and w, that is $R_{\|}/L \propto P^{\alpha}w^{\beta}$.[23] The width of the filament is ~8 nm, based on the medial distance in the HU–DNA network.[13] In a channel with an average cross-sectional diameter of 225 nm, the scaling exponent for P takes the value $\alpha = 0.62$. P can then be obtained from $P = P_{\circ}\left(R_{\|}/R_{\|}^{\circ}\right)^{1/\alpha}$, with $P_{\circ}$ and $R_{\|}^{\circ}$ being the persistence length and stretch in the protein-free state, respectively. The results calculated with $P_{\circ}$ = 55 nm are demarcated along the right-axes in Fig. 4. It should be noted that the thus obtained values of P are apparent values, because the stretch is also affected by longer range interactions such as protein-mediated bridging of distal segments of the DNA molecule. The temporary increase in stretch corresponds with an temporary increase in P to 125–175 nm with the larger value pertaining to the highest employed concentration of HU of 800 nM.

The apex in the stretch is reached in about 20 min. For longer exposure times, the stretch decreases and falls back to a value less than the value pertaining to HU-free DNA. This temporal behaviour differs from what has been observed before for H-NS. In the case of exposure to 800 nM of H-NS in otherwise the same experimental conditions, the stretch monotonously increases over a time span of 90 min.[23] Coating and filamentation of DNA with HU is hence markedly faster than with H-NS. As discussed above, the decrease in stretch can be related to two effects. The first effect is a decrease in P due to a structural rearrangement of the HU–DNA complex. This effect can however not explain a final value less than the one for HU-free DNA, because P was not observed to become less than $\sim$50 nm.[12] Accordingly, a second effect of HU mediated bridging interaction is required to reconcile our observation of contraction for equilibrated DNA after long exposure times.

An increased bending rigidity of the HU–DNA complex for HU concentrations exceeding 50 nM was previously reported based on the analysis of single molecule force-stretching experiments and atomic force microscopy images.[9,12,31] Force-stretching experiments showed a P value of around 150 nm at 800 nM HU.[9] The latter experiments are typically done within 15–30 min after exposure to HU. Accordingly, fair agreement is observed between the thus measured value of P and the one pertaining to the apex in the stretch (see Fig. 4B). Conversely, analysis of the motion of a particle tethered to a grafted DNA molecule without the application of force did not show an increase in P exceeding that of bare DNA.[32] The DNA molecule compacts irrespective of the concentration of HU. Several explanations for this contradictory result have been proposed in the literature, that are the microbial source of HU, the effect of stretching the substrate on HU binding, and structural rearrangement of bound HU on DNA.[12,32] Confinement inside a channel of 200 nm corresponds with a stretching force of around 0.02 pN.[33] Accordingly, we observed compaction at a minimal stretching force but for long enough incubation time. Quantitative differences might be related to differences in buffer composition and/or the source of HU.[11,34] The apparent persistent length does not exceed the one for bare DNA due to structural rearrangement of the complex in conjunction with protein-mediated bridging interaction.

4.3 Condensation of DNA by HU

For over-threshold concentrations of HU, the DNA molecules compact into a condensed form. Nanochannel-facilitated condensation of DNA by neutral crowders, like-charge proteins (hemoglobin and bovine serum albumin), and bacterial proteins H-NS and Hfq has been reported before.[19,22–25] For neutral crowders and like-charge proteins, the critical concentration for condensation is in the range of tens to hundreds of micromolars. In the case of the bacterial proteins, the critical concentrations are one or two orders of magnitude lower in the nano- to micromolar range. Among the investigated NAPs, Hfq is the most potent condensing agent. The total amount of Hfq in the bacterial cell is comparable to those of HU and H-NS, but only 10% is associated with the nucleoid.[35,36] Hfq's highest efficiency for condensation thus offsets a lower fraction of chromosome-bound protein. The critical concentrations for HU are similar or slightly less than the ones for H-NS, but for HU there is a stronger dependence on the medium ionic strength and/or the presence of magnesium ions. DNA filaments coated with HU assemble into a periodic network with $\sim$8 nm repeat distance in the medial direction.[13] A plausible explanation for compaction and condensation is hence HU-mediated bridging between (almost) parallel segments of the DNA molecule. Confinement inside a nanochannel imposes mutual alignment of segments of the DNA molecule, thereby increasing the attractive interaction resulting in compaction into the condensed form. Concurrently, the probability for segment juxtaposition is reduced due to the channel-induced linearisation of the DNA molecule. This reduction in segment juxtaposition results in a shift of the critical concentration for condensation towards higher values for smaller channel diameters. The strong dependence of the critical concentrations for condensation on the ionic composition and strength of the supporting medium is related to screening of electrostatic repulsion between the like-charged segments of the DNA molecule.

5 Conclusions

Our experiments confirm the previously reported time-dependence in the mechanical properties of the HU–DNA complex.[12] Initially, the molecules elongate due to the formation of the nucleoprotein filament. However, when time progresses the molecules contract and, eventually, an equilibrium state is reached with an extension less than the value pertaining to the protein-free state. This reduction in extension is related to a reduction in persistence length associated with a rearrangement of bound HU on DNA and HU mediated bridging interactions among distal DNA segments. For low enough HU concentrations, the molecules contract but they do not compact into a condensed form. A unique feature of the confinement in a nanospace is that the molecules do compact into a condensed form for over-threshold concentrations of bacterial proteins. This phenomenon is shared with neutral crowding agents as well as like charge proteins, but condensation induced by HU, Hfq or H-NS occurs at a much lower concentration in the nano- to micromolar range. Our results show that the effects of architectural proteins on the conformation and folding of DNA do not depend on DNA–protein interaction and crowding *per se*, but the interplay with the confinement in a nanospace such as within the nucleoid of a bacterial cell is of paramount importance.

Conflicts of interest

There are no conflicts to declare.

Acknowledgements

This research was supported by grant MOE2014-T2-1-001 of Singapore's Ministry of Education. Nora Goosen (Leiden University) is thanked for the gift of the HU expression vector.

References

1 T. A. Azam, A. Iwata, A. Nishimura, S. Ueda and A. Ishihama, *J. Bacteriol.*, 1999, **181**, 6361–6370.
2 N. E. Dixon and A. Kornberg, *Proc. Natl. Acad. Sci. U. S. A.*, 1984, **81**, 424–428.
3 L. Claret and J. Rouviere-Yaniv, *J. Mol. Biol.*, 1997, **273**, 93–104.
4 V. Pinson, M. Takahashi and J. Rouviere-Yaniv, *J. Mol. Biol.*, 1999, **287**, 485–497.
5 H. Tanaka, N. Goshima, K. Kohno, Y. Kano and F. Imamoto, *J. Biochem.*, 1993, **113**, 568–572.
6 K. K. Swinger, K. M. Lemberg, Y. Zhang and P. A. Rice, *EMBO J.*, 2003, **22**, 3749–3760.
7 K. K. Swinger and P. A. Rice, *J. Mol. Biol.*, 2007, **365**, 1005–1016.
8 I. Tanaka, K. Appelt, J. Dijk, S. W. White and K. S. Wilson, *Nature*, 1984, **310**, 376–381.
9 J. van Noort, S. Verbrugge, N. Goosen, C. Dekker and R. T. Dame, *Proc. Natl. Acad. Sci. U. S. A.*, 2004, **101**, 6969–6974.
10 R. T. Dame, *Mol. Microbiol.*, 2005, **56**, 858–870.
11 B. Xiao, R. C. Johnson and J. F. Marko, *Nucleic Acids Res.*, 2010, **38**, 6176–6185.
12 B. Kundukad, P. Cong, J. R. C. van der Maarel and P. S. Doyle, *Nucleic Acids Res.*, 2013, **41**, 8280–8288.
13 M. Hammel, D. Amlanjyoti, F. E. Reyes, J.-H. Chen, R. Parpana, H. Y. Tang, C. A. Larabell, J. A. Tainer and S. Adhya, *Sci. Adv.*, 2016, **2**, e1600650.
14 J. A. van Kan, A. A. Bettiol and F. Watt, *Nano Lett.*, 2006, **6**, 579–582.
15 J. A. van Kan, C. Zhang, P. P. Malar and J. R. C. van der Maarel, *Biomicrofluidics*, 2012, **6**, 036502.
16 C. Zhang, F. Zhang, J. A. van Kan and J. R. C. van der Maarel, *J. Chem. Phys.*, 2008, **128**, 225109.
17 J. R. C. van der Maarel, C. Zhang and J. A. van Kan, *Isr. J. Chem.*, 2014, **54**, 1573–1588.
18 K. Frykholm, L. K. Nyberg and F. Westerlund, *Integr. Biol.*, 2017, **9**, 650–661.
19 C. Zhang, P. G. Shao, J. A. van Kan and J. R. C. van der Maarel, *Proc. Natl. Acad. Sci. U. S. A.*, 2009, **106**, 16651–16656.
20 J. J. Jones, J. R. C. van der Maarel and P. S. Doyle, *Nano Lett.*, 2011, **11**, 5047–5053.
21 L. Dai, J. R. C. van der Maarel and P. S. Doyle, *ACS Macro Lett.*, 2012, **1**, 732–736.
22 C. Zhang, Z. Gong, D. Guttula, P. P. Malar, J. A. van Kan, P. S. Doyle and J. R. C. van der Maarel, *J. Phys. Chem. B*, 2012, **116**, 3031–3036.
23 C. Zhang, D. Guttula, F. Liu, P. P. Malar, S. Y. Ng, L. Dai, P. S. Doyle, J. A. van Kan and J. R. C. van der Maarel, *Soft Matter*, 2013, **9**, 9593–9601.
24 K. Jiang, C. Zhang, D. Guttula, F. Liu, J. A. van Kan, C. Lavelle, K. Kubiak, A. Malabirade, A. Lapp, V. Arluison and J. R. C. van der Maarel, *Nucleic Acids Res.*, 2015, **43**, 4332–4341.
25 A. Malabirade, K. Jiang, K. Kubiak, A. Diaz-Mendoza, F. Liu, J. A. van Kan, J.-F. Berret, V. Arluison and J. R. C. van der Maarel, *Nucleic Acids Res.*, 2017, **45**, 7299–7308.
26 W. Wang, G.-W. Li, C. Chen, X. S. Xie and X. Zhuang, *Science*, 2011, **333**, 1445–1449.
27 C. Zhang, K. Jiang, F. Liu, P. S. Doyle, J. A. van Kan and J. R. C. van der Maarel, *Lab Chip*, 2013, **13**, 2821–2826.
28 A. S. Krylov, O. A. Zasedateleva, D. V. Prokopenko, J. Rouviere-Yaniv and A. D. Mirzabekov, *Nucleic Acids Res.*, 2001, **29**, 2654–2660.
29 J. A. van Kan, P. G. Shao, Y. H. Wang and P. Malar, *Microsyst. Technol.*, 2011, **17**, 1519–1527.
30 J. O. Tegenfeldt, C. Prinz, H. Cao, S. Chou, W. W. Reisner, R. Riehn, Y. M. Wang, E. C. Cox, J. C. Sturm, P. Silberzan and R. Austin, *Proc. Natl. Acad. Sci. U. S. A.*, 2004, **101**, 10979–10983.
31 D. Skoko, B. Wong, R. C. Johnson and J. F. Marko, *Biochemistry*, 2004, **43**, 13867–13874.
32 G. Nir, M. Lindner, H. R. C. Dietrich, O. Girshevitz, C. E. Vorgias and Y. Garini, *Biophys. J.*, 2011, **100**, 784–790.
33 J. R. C. van der Maarel, *Introduction to Biopolymer Physics*, World Scientific, 2007.
34 A. Grove, *Curr. Issues Mol. Biol.*, 2011, **13**, 1–12.
35 T. A. Azam, S. Hiraga and A. Ishihama, *Genes Cells*, 2000, **5**, 613–626.
36 E. Diestra, B. Cayrol, V. Arluison and C. Risco, *PLoS One*, 2009, **4**, e8301.

